



Novel bicyclic pyrazoles as potent ALK2 (R206H) inhibitors for the treatment of fibrodysplasia ossificans progressiva

Hirofumi Yamamoto^a, Naoki Sakai^b, Satoshi Ohte^c, Tomohiro Sato^d, Katsuhiko Sekimata^{a,*}, Takehisa Matsumoto^b, Kana Nakamura^b, Hisami Watanabe^b, Chiemi Mishima-Tsumagari^b, Akiko Tanaka^b, Yoshinobu Hashizume^e, Teruki Honma^d, Takenobu Katagiri^f, Kohei Miyazono^g, Hiroshi Tomoda^c, Mikako Shirouzu^b, Hiroo Koyama^a

^a Drug Discovery Chemistry Platform Unit, RIKEN Center for Sustainable Resource Science, 2-1 Hirosawa, Wako, Saitama 351-0198, Japan

^b Drug Discovery Structural Biology Platform Unit, RIKEN Center for Biosystems Dynamics Research, 1-7-22 Suehiro-cho, Tsurumi-ku, Yokohama 230-0045, Japan

^c Department of Microbial Chemistry, Graduate School of Pharmaceutical Sciences, Kitasato University, 5-9-1 Shirokane, Minato-ku, Tokyo 108-8641, Japan

^d Drug Discovery Computational Chemistry Platform Unit, RIKEN Center for Biosystems Dynamics Research, 1-7-22 Suehiro-cho, Tsurumi-ku, Yokohama 230-0045, Japan

^e RIKEN Program for Drug Discovery and Medical Technology Platforms, 2-1 Hirosawa, Wako, Saitama 351-0198, Japan

^f Division of Biomedical Sciences, Research Center for Genomic Medicine, Saitama Medical University, 1397-1 Yamane, Hidaka-shi, Saitama 350-1241, Japan

^g Department of Molecular Pathology, Graduate School of Medicine, The University of Tokyo, 7-3-1 Hongo, Bunkyo-ku, Tokyo 113-0033, Japan

ARTICLE INFO

Keywords:

Fibrodysplasia ossificans progressiva (FOP)

Activin receptor-like kinase-2 (ALK2)

Bicyclic pyrazole derivatives

ABSTRACT

Mutant activin receptor-like kinase-2 (ALK2) is associated with the pathogenesis of fibrodysplasia ossificans progressiva, making it an attractive target for therapeutic intervention. We synthesized a new series of bicyclic pyrazoles and evaluated their mutant ALK2 enzyme inhibitory activities, leading to the identification of **8** as the most potent inhibitor. This compound showed moderate microsomal metabolic stability and human ether-a-go-go related gene (hERG) safety. In C2C12 cells carrying mutant ALK2 (R206H), **8** efficiently inhibited the bone morphogenetic protein (BMP)-induced alkaline phosphatase activity.

Fibrodysplasia ossificans progressiva (FOP) is a rare disorder that manifests as progressive heterotopic ossification in the muscles, tendons, or ligaments.^{1,2} FOP is caused by abnormal activation of bone morphogenetic protein (BMP) signaling due to highly recurrent mutations, including R206H in ALK2 (encoded by *ACVRI*), one of the type-I receptors for BMPs, resulting in an alteration in the intracellular glycine-serine-rich domain of the enzyme.^{1,2} Another disease caused by ALK2 mutations, including ALK2 (R206H), is diffuse intrinsic pontine glioma (DIPG), a fatal cancer that forms in the brainstem of children.^{2,3} Thus, the inhibition of the BMP signaling pathway, which acts on ALK2 (R206H), may be an effective treatment for FOP and/or DIPG.²

While some ALK2 inhibitors have been shown to be efficacious in disease animal models of FOP and DIPG, only BLU-782, saracatinib, and KER-047 are currently under clinical trials for treating FOP.^{2,4-10} Therefore, the development of novel and specific ALK2 mutant

inhibitors may compensate for the lack of drug candidates and provide a further proof-of-concept of ALK2 inhibition for these diseases. Previously, we reported a series of bis-heteroaryl pyrazoles as hit ALK2 inhibitors exemplified by RK-59638 (Fig. 1).^{11,12}

X-ray crystal structure analysis showed that RK-59638 binds to the ALK2 (R206H) ATP binding pocket (PDB code 6ACR) (Fig. 1).^{11,12} The pharmacophore of RK-59638 was found to be characterized by two chemical features: an aminopyrimidine hinge binder and 3-pyridyl back pocket binder. Additionally, the methoxy group of the anisidine moiety is exposed to the solvent region. The pyrazole moiety is located in the sugar pocket of the enzyme. In contrast, fused morpholinopyrazole motifs are expected to affect the activities of these compounds by the CH- π interaction with Tyr219 on the phosphate-binding loop (P loop) and by a water-mediated hydrogen bond network with Ser290 and Asp293 (Fig. 1).

Abbreviations: ALK2, activin receptor-like kinase-2; ALP, alkaline phosphatase; BMP, bone morphogenetic protein; DIPG, diffuse intrinsic pontine glioma; DMF, *N,N*-dimethylformamide; FOP, fibrodysplasia ossificans progressiva; Herg, human ether-a-go-go related gene; MDCK, Madin-Darby canine kidney cells; SAR, structure-activity relationship.

* Corresponding author.

E-mail address: katsuhiko.sekimata@riken.jp (K. Sekimata).

<https://doi.org/10.1016/j.bmcl.2021.127858>

Received 27 November 2020; Received in revised form 1 February 2021; Accepted 5 February 2021

Available online 18 February 2021

0960-894X/© 2021 Elsevier Ltd. All rights reserved.

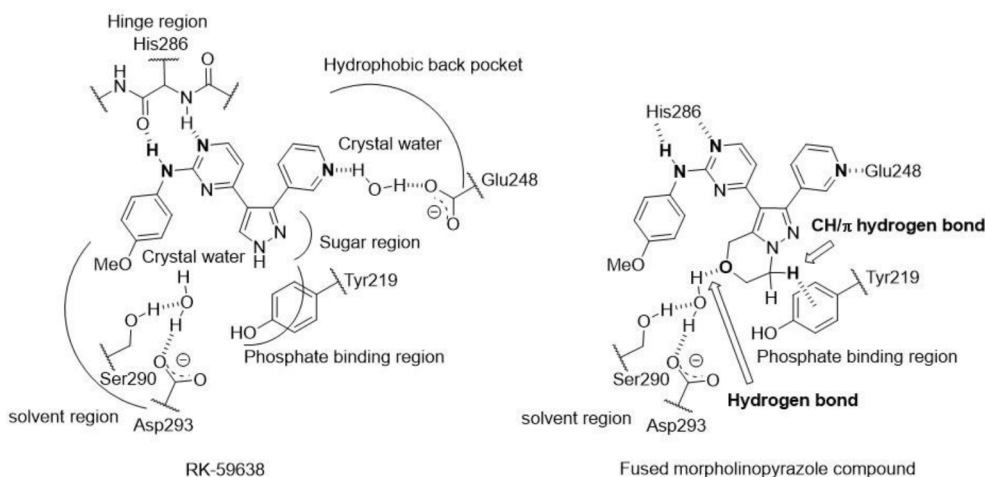


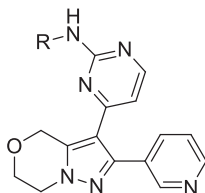
Fig. 1. Schematic 2D representation of the binding mode of RK-59638 in ALK2 (R206H) and our predicted binding mode of fused morpholinopyrazole **1** in ALK2 (R206H).

In this study, we identified a series of novel bicyclic pyrazole ALK2 (R206H) inhibitors by chemical modification of hit RK-59638. We also evaluated the effects of representative compounds on the differentiation

of mouse myoblastic C2C12 cells into osteoblasts by measuring the inhibition of BMP-induced alkaline phosphatase (ALP) activity, which is a marker of osteoblast differentiation.¹³

Table 1

Inhibition of ALK2 (R206H) enzyme activity, permeability, and efflux profiles.



Cpd No.	R	% inhibition at 0.3 μM ^{a,b,c}	IC ₅₀ (μM) ^{b,c,d}	Permeability Papp A to B (10^{-6} cm/s) ^{c,e}	Efflux ratio B to A/A to B MDR (B to A/A to B) ^{c,e}
RK-59638	–	38.8	0.684	NT	NT
1		NT	0.167	NT	NT
2		58.0	NT	NT	NT
3		–3.9	NT	NT	NT
4		73.0	NT	NT	NT
5		NT	0.0658	NT	NT
6		NT	0.0217	0.906	10.2 (53.9)
7		NT	0.0247	4.366	1.4 (6.1)
8		NT	0.0182	8.686	1.6 (5.8)

^a ALK2(R206H) enzyme assays were conducted by Reaction Biology Corporation using the 'HotSpot' assay platform and kinase Assay Protocol. Measured at ATP concentration (10 μM); for experimental details, see Ref. ¹¹.

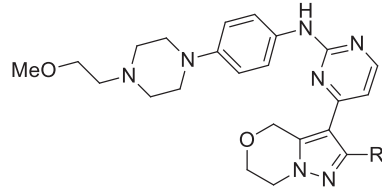
^b The percent inhibition values are the averages of two or more tests.

^c NT, not tested.

^d IC₅₀ values are the averages of two or more tests.

^e These studies were conducted by Sumika Chemical Analysis Service, Ltd. (SCAS) using *in vitro/vivo* pharmacokinetic screening.¹¹

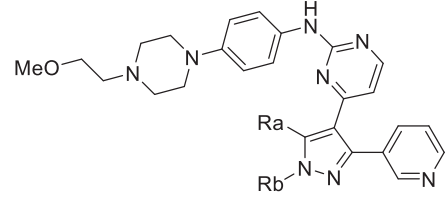
Table 2
Inhibition of ALK2 (R206H) enzyme activity.¹¹



Cpd No.	R	IC ₅₀ (nM) ^a
8		18.2
9		276
10		665
11		2890

^a IC₅₀ values are the averages of two or more tests.

Table 3
Inhibition of ALK2 (R206H) enzyme activity.¹¹



Cpd No.	Ra-Rb	IC ₅₀ (nM) ^a
8	CH ₂ OCH ₂ CH ₂	18.2
12	CH ₂ CH ₂ CH ₂	28.9
13	CH ₂ (CH ₂) ₂ CH ₂	24.9

^a IC₅₀ values are the averages of two or more tests.

To study the activity of fused morpholinopyrazole compound, we performed molecular docking simulations using the ALK2 (R206H) and RK-59638 (PDB code 6ACR) based on the GLIDE SP mode.¹⁴ The docked model for RK-59638 agreed well with the reported crystal structure coordinates. The binding mode and score of fused morpholinopyrazole **1** were analyzed in comparison to RK-59638. Compound **1** adopted the same binding mode as RK-59638. The docking scores of RK-59638 and **1** were -8.5123 and -8.9590 , respectively. As shown by docking analysis, **1** exhibited a four-fold increase in enzyme inhibitory activity compared to RK-59638, suggesting that the fused ring is important for the interaction with ALK2 (R206H) (Table 1). Compound **1** was then further optimized. In the structure-activity relationship (SAR) of solvent-exposed anisidine moiety, *para*-substituted **1** and **4** exhibited substantial levels of activity, whereas *meta*-substituted **2** and *ortho*-substituted **3** showed decreased activity (Table 1). Saturated heterocyclic **5** and **6**, containing oxygen or nitrogen at the end of the structure, were found to be mildly and highly potent, respectively. Piperazine **6** showed low permeability (A to B Papp = 0.906×10^{-6} cm/s) and a high efflux ratio (53.9), which was greater than the efflux ratio (46.0) of digoxin, a known substrate of MDR1, in MDR1-MDCKII cell (Table 1). Low efflux has been shown to be important for achieving sufficient exposure in rat.¹¹ The high efflux ratio of **6** was improved by capping the NH group of the piperazine moiety of **6** as an *N*-methyl group (**7**) and *N*-methoxyethyl group (**8**) (Table 1). Compound **8** showed the strongest enzyme

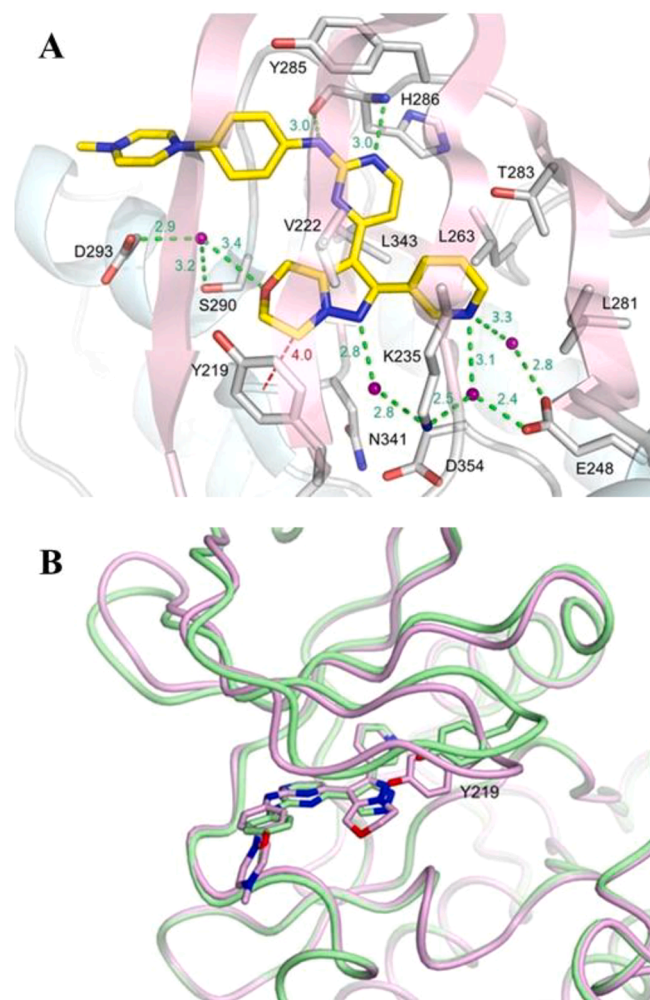


Fig. 2. (A) Binding mode of **7** in the ATP sites of ALK2 (R206H). Secondary structure elements of ALK2 (R206H) are represented by ribbon model. Residues forming ATP-binding pocket are shown as white stick model. Compound **7** is represented by yellow stick model. The hydrogen bonds involved in the interaction of ALK2 (R206H) and **7** are shown in green dashed line. Water molecules are shown as purple sphere. (B) Superposition of the ALK2 (R206H)—RK-59638 complex (green) and ALK2 (R206H)—**7** complex (purple).

Table 4
Chemical profiles of RK-59638 and **8**.

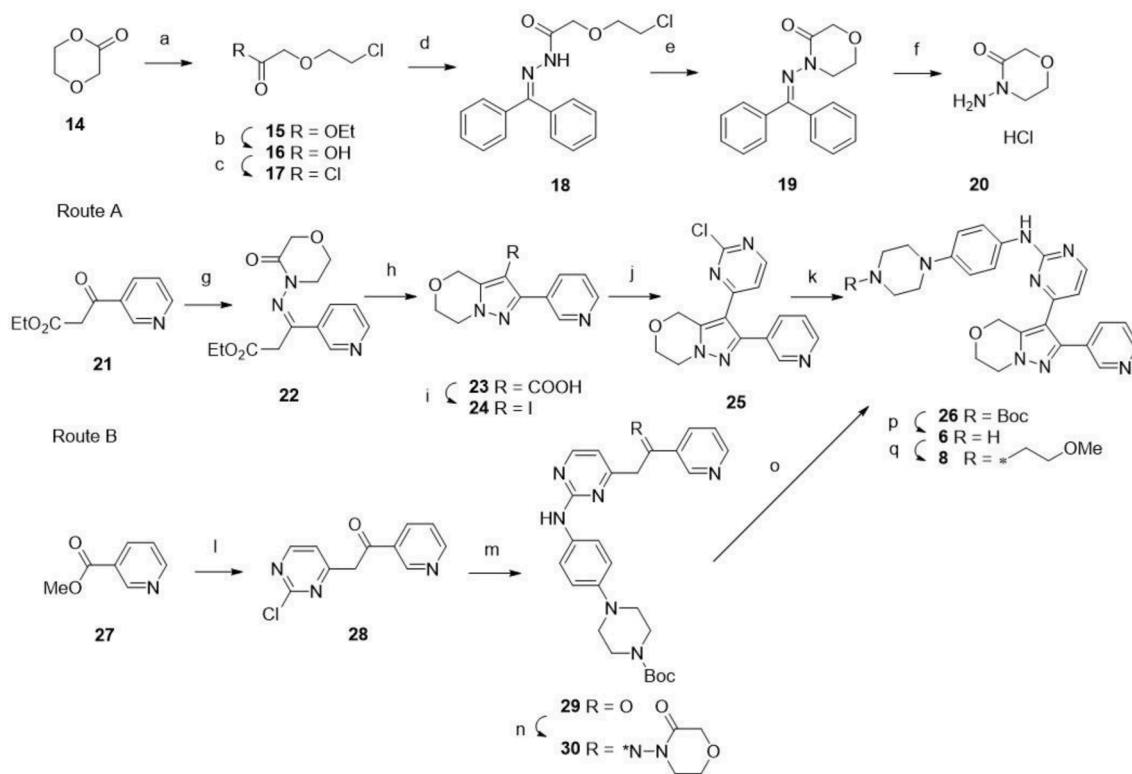
		RK-59638	8
Biochemical	IC ₅₀ ALK2 (R206H) (nM) IC ₅₀ ALK2 (R206H) (nM)	683.7	18.2
Cellular	IC ₅₀ ALP (nM) ^a	>100	37.3
Metabolic stability	HLM/RLM (% remaining after 60 min) ^b	14.8/2.1	56.0/40.5
hERG	Automated patch-clamp (% inhibition at 10 μM) ^c	25.4	3.6

^a Details of ALP assays using C2C12 cells carrying mutant ALK2 (R206H) were described previously.^{15,16} IC₅₀ values are the averages of two or more tests.

^b These studies were conducted by Sumika Chemical Analysis Service, Ltd. (SCAS) using *in vitro/vivo* pharmacokinetic screening.

^c These studies were conducted by Cerep, Ltd. using *in vitro* ADME.

inhibitory activity, considerable permeability, and acceptable P-gp-mediated efflux. To explore the SAR of the 3-pyridyl moiety of **8** surrounded by the hydrophobic back pocket of the enzyme, the pyridine moiety was replaced with a phenyl or heteroaryl (Table 2). Compounds



Scheme 1. Reagents and conditions: (a) SOCl_2 , ethanol, quant; (b) NaOH, tetrahydrofuran, 90%; (c) SOCl_2 , DMF, 88%; (d) (Diphenylmethylene)hydrazine, pyridine, CH_2Cl_2 , 99%; (e) NaH, tetrahydrofuran, 83%; (f) HCl aq, 88%; (g) 20, pyridine, ethanol, 59%; (h) Sodium ethoxide, toluene, 74%; (i) *N*-iodosuccinimide, NaHCO_3 , DMF, 77%; (j) 2-Chloro-4-(tributylstannyl)pyrimidine, $\text{Pd}(\text{PPh}_3)_4$, CuI, DMF, 59%; (k) 4-(4-Boc-piperazin-1-yl)aniline, Methanol, tetrahydrofuran, 56%; (l) 2-chloro-4-methylpyrimidine, lithium hexamethyldisilazide, 73%; (m) 1-Boc-4-(4-aminophenyl)piperazine, 43%; (n) 20, pyridine, ethanol, 74%; (o) NaH, DMF, 43%; (p) Trifluoroacetic acid, CH_2Cl_2 , 80%; (q) 1-bromo-2-methoxyethane, *N,N*-diisopropylethylamine, acetonitrile, 72%.

9–11 showed significant decreases in enzyme inhibitory activity, suggesting that the 3-pyridyl group is essential for interacting with the enzyme. Finally, the fused bicyclic pyrazole moiety of **8** was optimized. The results showed that the IC_{50} value of alicyclic type **12** and **13** were lower than that of **8** (Table 3). X-ray crystallographic analyses were conducted to examine the SAR in a structural context. It was expected that soaking **8** would be difficult because the *N*-methoxyethyl group of **8** caused a steric clash with a neighboring protomer in the crystal. Thus, **7** possessing the *N*-methyl group was selected for crystal structure analysis. A previous study revealed that **7** directly binds to the ALK2 (R206H) ATP-binding pocket in the same manner as RK-59638 (PDB code 6ACR) (Fig. 2A).

Compound **7** formed two hydrogen bonds between the aminopyrimidine moiety and the main chain amine and carbonyl of the His286 in the hinge region of the enzyme. Three hydrogen bonds were formed between the nitrogen of the 3-pyridyl group of **7**, the carboxyl group of Glu248 from the α C helix, and the amino group of Lys235 from the β 3 strand via conserved water molecules. A hydrogen bond was formed between the nitrogen of the pyrazole ring of **7** and the amino group of Lys235 via a conserved water molecule. Another weak hydrogen bond might have formed between the oxygen atom of the morpholinopyrazole moiety of **7** and Asp293 and Ser290 via a conserved water molecule. The oxygen atom and the water molecule were 3.4 Å apart. Moreover, the morpholine moiety was located near Tyr219. The methylene carbon atoms at the morpholine moiety and the aromatic ring of Tyr219 were 4.0 Å apart, and they formed a CH- π interaction. Structural superposition of RK-59638 and **7** showed that the fused morpholinopyrazole motif of **7** induced a significant positional change in Tyr219 on the P loop (Fig. 2B), suggesting that the motif is important for CH- π interaction with Tyr219 in ALK2 (R206H).

In addition to the biochemical ALK2 (R206H) assay, RK-59638 and **8**

were evaluated in ALK2 (R206H) – expressing C2C12 cells to determine their ability to inhibit BMP4-induced ALP activity.^{15,16} ALP is a useful biochemical marker of osteoblastic differentiation of C2C12 cells.¹³ Compound **8** showed higher potency than RK59638, which was consistent with the biochemical ALK2 (R206H) assay (Table 4). Moreover, **8** showed improvements in human and rat microsomal stability and reduced the human ether-a-go-go related gene (hERG) inhibition compared with RK-59638 (Table 4).

The synthesis of **8** was achieved via two divergent routes: route A included the Stille cross-coupling reaction and route B included a nucleophilic substitution reaction using lithium hexamethyldisilazide (Scheme 1).

First, key intermediate **20** was synthesized. Commercially obtained *p*-dioxanone **14** was treated with thionyl chloride in ethanol to give the corresponding ethyl ester **15**.¹⁷ Carboxylic acid **16** was formed by base hydrolysis of **15** and then treated with thionyl chloride in *N,N*-dimethylformamide (DMF) to give the corresponding acid chloride **17**.¹⁷ Compound **17** was coupled using benzophenone hydrazine with pyridine to give the amide product **18**.¹⁸ Compound **19** was obtained by intramolecular dehydrohalogenation of **18** with sodium hydride in tetrahydrofuran, followed by deprotection using aqueous hydrochloric acid to give the intermediate **20**.¹⁸ Next, as shown in Scheme 1, for route A, commercially obtained 3-oxo-3-(pyridin-3-yl)propionic acid ethyl ester **21** was condensed with the hydrazide **20** in pyridine to give the corresponding acyl hydrazone **22**.¹⁹ Compound **22** was cyclized and hydrolyzed using sodium ethoxide to give carboxylic acid **23**. Acid **23** was treated with *N*-iodosuccinimide in DMF at 25 °C to give the corresponding iodide **24**.¹⁸ The Stille reaction of iodide **24** with 2-Chloro-4-(tributylstannyl)pyrimidine produced chloride **25**. Displacement of the chloride **25** with 1-Boc-4-(4-aminophenyl)piperazine gave **26**.¹¹ As shown in Scheme 1, for route B, commercially available methyl

nicotinate **27** was reacted with the lithium enolate of 2-chloro-4-methylpyrimidine to give ketone **28**.¹¹ Displacement of the chloride **28** with 1-Boc-4-(4-aminophenyl)piperazine and subsequent condensation with hydrazide **20** in pyridine gave the corresponding acyl hydrazone **30**.¹⁹ Compound **30** was cyclized using sodium hydride to give **26**. Finally, Boc-deprotection of **26** using trifluoroacetic acid gave **6** and subsequent reaction of **6** with 1-bromo-2-methoxyethane and *N,N*-diisopropylethylamine in DMF gave **8**.

In summary, we have identified a highly potent ALK2 (R206H) inhibitor **8** showing good membrane permeability, strong ALP inhibitory activity in C2C12 (R206H) cells, moderate microsomal metabolic stability, and moderate hERG safety. In our future studies, the compound **8** and its derivatives will be evaluated for their pharmacokinetics profile using *in vitro* ADME/Tox assays, and their *in vivo* efficacies in animal models of FOP and /or DIPG.

Declaration of Competing Interest

The authors declare the following financial interests/personal relationships which may be considered as potential competing interests: Takenobu Katagiri receives research support from Daiichi-Sankyo, Co. Ltd. The other authors declare no competing interest in the present study.

Acknowledgements

We thank Dr. H. Kojima (Drug Discovery Initiative, The University of Tokyo) for providing the chemical library. This work was partially supported by the Platform Project for Supporting in Drug Discovery and Life Science Research from Japan Agency for Medical Research and Development (AMED). This work was supported by RIKEN Program for Drug Discovery and Medical Technology Platforms.

Appendix A. Supplementary data

Supplementary data to this article can be found online at <https://doi.org/10.1016/j.bmcl.2021.127858>.

References

- 1 Pignolo RJ, Shore EM, Kaplan FS. *Pediatr Endocrinol Rev.* 2013;10:437–448.
- 2 Sekimata K, Sato T, Sakai N. *Chem Pharm Bull.* 2020;68:194–200.
- 3 Taylor KR, Mackay A, Truffaux N, et al. *Nat Genet.* 2014;46:457–461.
- 4 Yu PB, Deng DY, Lai CS, et al. *Nat Med.* 2008;14:1363–1369.
- 5 Mohedas AH, Xing X, Armstrong KA, et al. *ACS Chem Biol.* 2013;8:1291–1302.
- 6 Hoeman CM, Cordero FJ, Hu G, et al. *Nat Commun.* 2019;10:1023.
- 7 Carvalho D, Taylor KR, Olaciregui NG, et al. *Commun Biol.* 2019;2:156.
- 8 A Phase 1, randomized, double-blind, placebo-controlled, single and multiple ascending dose and food effect study to evaluate the safety, tolerability, and pharmacokinetics of BLU-782 when administered orally to healthy adult subjects. Available at: <<https://clinicaltrials.gov/ct2/show/NCT03858075?term=BLU-782&draw=2&rank=1>> [Last accessed Jan 24, 2021].
- 9 Saracatinib trial TO prevent FOP. Available at: <<https://clinicaltrials.gov/ct2/show/NCT04307953?term=AZD0530&draw=2&rank=2>> [Last accessed Jan 24, 2021].
- 10 Randomized, double-blind, placebo-controlled, single and multiple ascending dose study to evaluate the safety, tolerability and pharmacokinetics of KER-047 administered to healthy male volunteers and postmenopausal female volunteers. Available at: <<https://www.anzctr.org.au/Trial/Registration/TrialReview.aspx?id=376969>> [Last accessed Jan 24, 2021].
- 11 Sekimata K, Sato T, Sakai N, et al. *Chem Pharm Bull.* 2019;67:224–235.
- 12 Sato T, Sekimata K, Sakai N, et al. *ASC Omega.* 2020;5:11411–11423.
- 13 Katagiri T, Yamaguchi A, Komaki M, et al. *J Cell Biol.* 1994;127:1755–1766.
- 14 GLIDE. Schrödinger Inc., New York, NY, USA, <http://www.schrodinger.com/>.
- 15 Fukuda T, Kohda M, Kanomata K, et al. *J Biol Chem.* 2009;284:7149–7156.
- 16 Ohte S, Shokawa T, Koyama N, et al. *J Antibiot.* 2020;73:554–558.
- 17 Eickmeier C, Fuchs K, Peters S, et al. WO 2006/103038; 2006.
- 18 Sawyer JS, Beight DW, Ciapetti P, et al. WO 2002/094833; 2002.
- 19 Li HY, Wang Y, McMillen WT, et al. *Tetrahedron.* 2007;63:11763–11770.